Analytical Modeling Concept for Weather Phenomena as Renewable Energy Resources

Franz Christange
Chair of Renewable and Sustainable Energy Systems
Technical University of Munich
80333 Munich, Germany
Email: franz.christange@tum.de

Thomas Hamacher
Chair of Renewable and Sustainable Energy Systems
Technical University of Munich
80333 Munich, Germany
Email: thomas.hamacher@tum.de

***Abstract*—This work describes a general concept for modeling weather phenomena as renewable energy resources. The model considers all typical effects, like time-variance, realistic rates of change, the causality relation between different weather phenomena and satisfying the reference distribution functions. The focus of this work is to design a continuous model, similar to a weather generator, with a simple analytical description. This paper illustrates the concept by a specific implementation for global horizontal irradiance, air temperature and wind speed. We describe the model itself and the data analysis to determine the model parameters. This specific implementation and the concept is validated by designing a model from a 8 year reference dataset. The results show a similar behavior to the recorded data. Only rare, extreme phenomenas are modeled limitedly.**

I. Introduction

This paper investigates modeling renewable energy resources (RER). Renewable power generation highly depends on the RERs which are finally weather effects, like the wind speed or the irradiance. One of the fundamental properties of weather effects is their fluctuating nature. The fluctuating RERs affect negatively the reliability of renewable energy systems (RES). To investigate such effects RES are modeled and analyzed. The resulting models are based on RER, which are either synthesized by a weather generator or recorded time series are used. The goal of this work is to develop a compact description of weather data for RER modeling which can be used for different applications.

Literature distinguishes two fundamentally different approaches to model weather data, the concept of weather generators and numerical global climate models [1]. The main difference is that weather generators are computationally fast and focus on small spatial areas, in contrast to the simulation of the whole atmosphere and the interaction with parts of the earth in a global view. For the purpose of modeling renewable energy systems, weather generators are the preferred option.

Weather generators are based on numerous fundamentally different methodological concepts. A common concept is to use Markov chains [2] [3] [4] to model the stochasticity of the data generation process. This concept is called sequential because Markov chains introduce a temporal correlation of the generated values. Temporal correlation means that the values of the time series depend on their prior values. Nonsequential methods depend on stochastic uncorrelated time series which are adjusted by the distribution function [5]. Other works are based on discrete states to incorporate a temporal correlation, by clustering specific weather phenomena [4], or to incorporate time-variance, like the seasonality by distinguishing the four seasons [6].

Weather models are used for generating weather data (e.g. [2]) and for forecast (e.g. [7]). In [7] the authors motivate their work on weather generators with investigating the propagation of wild fire. An often investigated topic is the reliability of technical facilities, like the electrical power distribution system [4]. For agricultural investigations the precipitation is a major element of weather generators [8]. Weather generators are used in renewable energy systems in [5], especially for photovoltaic [6] and wind power generation [2].

The goal for this paper is to develop a general concept for modeling renewable weather data and its specific implementation. The specific implementation models global horizontal irradiance, air temperature and wind speed, which serve as typical input data for photovoltaic and wind power models. The general concept targets the following requirements:

Analytical model: One of the major goals of this modeling concept is to achieve an analytical description of the model. Background for this requirement is to be able to use the analytical model for a detailed analysis of the potential of renewable energies and for system designs.

Simple model: The mathematics of the model have to be simple. Simplicity in this context means that the global behavior is modeled by stochastic processes to avoid to include complex deterministic processes as used for numerical global climate models. This requirement goes hand in hand with lower requirements on accuracy, so that this model is not to be meant to be used for forecast.

Time-variance: A further major requirement is to consider time-variance, which means the seasonal and diurnal variations, caused by the earth's movement.

Rate of change: An important model requirement is to incorporate that each RER features a typical rate of change behavior which results in the typical duration of certain weather phenomena. This means that there is a temporal correlation between the RER model values and their prior values.

Causality: There is a causal relation between each RER. A typical example is that irradiance causes an increasing temperature. Finally the model of the RER have to depend stochastically on each other. A typical example is that high irradiance results often, but not necessarily, in high temperature.

II. Analytical Modeling Concept

This section describes the analytical modeling concept for modeling N RER-time series x_n, which renewable energy system models depend on. The index $n \in [1, N]$ indicates the different time series like wind velocity or irradiance. The time series x_n are in general not normally distributed and their domains of definition $\mathbb{X}_n$ are in general not equal to real numbers $\mathbb{R}$. To be independent of the different types of distribution functions with their different domains of definition we assume a space χ with the real numbers $\mathbb{R}$ as the domain of definition and its values to be normally distributed. A final mapping maps the space χ to the RER-time series x_n.
The model is based on stochastic time series of time-invariant standard normally distributed ($\mathcal{N}(0,1)$) random values χ'_n, being time discrete white noise with sampling time T_S. The N white noise variables χ'_n are combined to one vector

$$\underline{\chi}' = (\chi'_1 \cdots \chi'_n \cdots \chi_N)^T \tag{1}$$

which is the fundamental input to the RER model.

The **rate of change** and the **causality** requirements are both addressed by one differential equation. The rate of change of the RER is addressed by the differential operator, which results in the differential equation. We assume a causality from RER $1 \ldots (n-1)$ to RER n, which defines the chronological order of n. Incorporating the causality and the rate of change leads to the correlated noise signal χ''_n. Its differential $\dot{\chi}''_n$ depends on the correlated noise signal χ''_n to model the rate of change, on the stochastic input χ'_n and on the noise signals $\chi'_1 \cdots \chi'_{(n-1)}$ to model the causality. The differential equations result in

$$\dot{\chi}''_n \quad = \quad f_n(\chi'_n, \chi'_1 \cdots \chi'_{n-1}). \tag{2}$$

The resulting correlated noise signals χ''_n are auto- and cross-correlated colored $\mathcal{N}(0,1)$-noise. The $\mathcal{N}(0,1)$-distribution has to be ensured by the differential equation in (2).

To include the **time-variance** into the RER model, we assume to know the time-variant mean $\underline{\mu}(t)$ and the time-variant standard deviation $\underline{\sigma}(t)$ of the normally distributed time series $\underline{\chi}$ which results in

$$\underline{\chi} = \underline{\chi}''\underline{\sigma}(t) + \underline{\mu}(t). \tag{3}$$

The deterministic time-variance of the RER model, modeled by $\underline{\mu}(t)$ and $\underline{\sigma}(t)$, depends on two frequency components: the diurnal and the seasonal variation with its harmonics. The diurnal variation is based on a daily periodicity with the frequency $\omega^\mathrm{d} = \frac{\pi}{12}\,{}^1\!/_\mathrm{h}$, and the seasonal variation on a yearly periodicity $\omega^\mathrm{y} = \frac{\pi}{4380}\,{}^1\!/_\mathrm{h}$.

Periodic signals can be described as a cosine series expansion, the Fourier series. In general, a periodic signal z is completely described by its fundamental frequency, amplitudes $A_0(s)$ and $A_k(s)$ and the phases $\varphi_k(s)$. The indices 0 and $k \in (1 \ldots \infty)$ refer to the order of the harmonics.

The yearly and daily periodicities of the mean $\underline{\mu}(t)$ and standard deviation $\underline{\sigma}(t)$ are separated because of the distinct fundamental frequencies $\omega^\mathrm{d} >> \omega^\mathrm{y}$. In the scope of one day, the yearly periodicity is neglected and we describe the diurnal variation through the Fourier series

$$\underline{z}(t) = \underline{A}^\mathrm{d}_0(\underline{z}(t)) + \sum_{k=1}^{\infty} \underline{A}^\mathrm{d}_k(\underline{z}(t)) \cdot \cos(k\underline{\omega}^\mathrm{d}t + \underline{\varphi}^\mathrm{d}_k(\underline{z}(t))) \tag{4}$$

for $\underline{z}(t) \in \{\underline{\mu}(t), \underline{\sigma}(t)\}$ and $\underline{\omega}^\mathrm{d} = (\omega^\mathrm{d} \ldots \omega^\mathrm{d})^T$ with $\dim(\underline{\omega}^\mathrm{d}) = N$.

In the scope of one year, the Fourier parameters of the daily scope (4) $\underline{A}^\mathrm{d}_0(\underline{z}(t))$, $\underline{A}^\mathrm{d}_k(\underline{z}(t))$ and $\underline{\varphi}^\mathrm{d}_k(\underline{z}(t))$ are yearly periodic and hence modeled by a further Fourier series

$$\begin{aligned} \underline{A}^\mathrm{d}_{k'}(\underline{z}(t)) \;&=\; \underline{A}^\mathrm{y}_0(\underline{A}^\mathrm{d}_{k'}(\underline{z}(t))) + \\ &\quad \sum_{l=1}^{\infty} \underline{A}^\mathrm{y}_l(\underline{A}^\mathrm{d}_{k'}(\underline{z}(t))) \cos(l\underline{\omega}^\mathrm{y}t + \underline{\varphi}^\mathrm{y}_l(\underline{A}^\mathrm{d}_{k'}(\underline{z}(t)))) \end{aligned} \tag{5}$$

$$\begin{aligned} \underline{\varphi}^\mathrm{d}_k(\underline{z}(t)) \;&=\; \underline{A}^\mathrm{y}_0(\underline{\varphi}^\mathrm{d}_k(\underline{z}(t))) + \\ &\quad \sum_{l=1}^{\infty} \underline{A}^\mathrm{y}_l(\underline{\varphi}^\mathrm{d}_k(\underline{z}(t))) \cos(l\underline{\omega}^\mathrm{y}t + \underline{\varphi}^\mathrm{y}_l(\underline{\varphi}^\mathrm{d}_k(\underline{z}(t)))) \end{aligned} \tag{6}$$

for $k' \in (0, k)$ and $\underline{\omega}^\mathrm{y} = (\omega^\mathrm{y} \ldots \omega^\mathrm{y})^T$ with $\dim(\underline{\omega}^\mathrm{y}) = N$. The resulting Fourier parameters are constant model parameters.

The last step of the modeling concept is the **transformation** $\underline{T}$ of the values $\underline{\chi}$ to the resulting RER-time series

$$\underline{x} = \underline{T}(\underline{\chi}). \tag{7}$$

This transformation maps the normal distribution of $\underline{\chi}$ to the distribution of $\underline{x}$. It has to be designed specifically, including the characteristics of each individual RER.

III. Modeling Weather Data

This section describes the modeling of global horizontal irradiance $\mathcal{I}$, air temperature $\mathcal{T}$ and wind speed $\mathcal{W}$, based on the previous introduced concept, with $N = 3$. Regarding the causality we assume that irradiance causes temperature, which causes wind speed, leading to the order

$$\underline{x} = \begin{pmatrix} \mathcal{I} & \mathcal{T} & \mathcal{W} \end{pmatrix}^T \tag{8}$$

resulting in the redefined index $n \in (\mathcal{I}, \mathcal{T}, \mathcal{W})$. This section describes the model of these RER-time series and how to analyze measured time series to obtain this model separately.

A. Apply RER model: time series synthesis

The model for the global horizontal irradiance $\mathcal{I}$, air temperature $\mathcal{T}$ and wind speed $\mathcal{W}$ are based on the concept of Sec. II. The model input is the 3-dimensional white noise vector $\underline{\chi}' = (\chi'_\mathcal{I}\ \chi'_\mathcal{T}\ \chi'_\mathcal{W})^T$ (1) to which we apply the dynamical equation (2). The goal is to obtain a simple dynamical equation to model the **rate of change** and the **causality**. We assume the

dynamics of a first order low pass system with a gain parameter B_n and a time constant T_n for all weather phenomena. The dynamics of the irradiance results in

$$\chi''_{\mathcal{I}} = \frac{B_{\mathcal{I}}}{1+T_{\mathcal{I}}s}\chi'_{\mathcal{I}} \tag{9}$$

with the Laplacian frequency parameter s.

The temperature $\mathcal{T}$ depends on the irradiance $\mathcal{I}$, and the windspeed $\mathcal{W}$ depends on the temperature $\mathcal{T}$, but shifted in time through the low pass filter with different time constants T_n. This dependency is modeled by the correlation factor $\zeta_n \in [0, \infty[$ through

$$\chi''_n = \frac{B_n}{1+T_n s}\frac{\zeta_n\chi'_{n-1}+\chi'_n}{\zeta_n+1} \quad \forall n \in (\mathcal{T},\, \mathcal{W}). \tag{10}$$

The correlated variables χ''_n (9), (10) are $\mathcal{N}(0,1)$-distributed. To ensure this, the filters $\frac{B_n}{1+T_n s}$ have to be standardized ($\frac{\zeta_n\chi_{n-1}+\chi_n}{\zeta_n+1}$ is already standardized) for their white noise input which leads with the sampling time T_S to

$$B_n = \sqrt{\frac{2T_n}{T_\mathrm{S}}}. \tag{11}$$

The next step is to include the **time-variance** through (3), which is described by (4)-(6). This mathematical exact description is simplified by considering only constant and first order harmonics. We introduce a more compact spelling of the Fourier parameters by writing the arguments into the index, resulting exemplary in $A_{0\varphi 1zn} = A_0^{\mathrm{y}}(\varphi_1^{\mathrm{d}}(z_n(t)))$, $A_{1zn}(t) = A_1^{\mathrm{d}}(z_n(t))$ or $\varphi_{1A0\sigma\mathcal{T}} = \varphi_1^{\mathrm{y}}(A_0^{\mathrm{d}}(\sigma_{\mathcal{T}}(t)))$ for $z \in (\mu, \sigma)$. The time-variance (4)-(6) leads to

$$\begin{aligned}
z_n(t) &= A_{0zn}(t) + A_{1zn}(t)\cdot\cos(\omega^{\mathrm{d}}t + \varphi_{1zn}(t)) && (12)\\
A_{0zn}(t) &= A_{0A0zn} + A_{1A0zn}\cdot\cos(\omega^{\mathrm{y}}t + \varphi_{1A0zn})) && (13)\\
A_{1zn}(t) &= A_{0A1zn} + A_{1A1zn}\cdot\cos(\omega^{\mathrm{y}}t + \varphi_{1A1zn})) && (14)\\
\varphi_{1zn}(t) &= A_{0\varphi 1zn} + A_{1\varphi 1zn}\cdot\cos(\omega^{\mathrm{y}}t + \varphi_{1\varphi 1zn})). && (15)
\end{aligned}$$

We **transform** the time-variant colored noise signal χ_n according to (7) to the RER-time series $\underline{x} = \begin{pmatrix}\mathcal{I} & \mathcal{T} & \mathcal{W}\end{pmatrix}^T$. The transformation of the irradiance $\mathcal{I}$ is based on a ratio η which accepts values between 0 and 1. This ratio η describes the proportion of the actual irradiance $\mathcal{I}$ by the maximum possible irradiance $\mathcal{I}_{\max}(t)$ resulting in

$$\mathcal{I} = T_{\mathcal{I}}(\chi_{\mathcal{I}}) := \eta(\chi_{\mathcal{I}})\cdot\mathcal{I}_{\max}(t). \tag{16}$$

The maximum possible irradiance $\mathcal{I}_{\max}(t)$ is computed by [9]

$$\mathcal{I}_{\max}(t) = \max\left(0,\ E_\mathrm{g}\cdot(\sin\phi\sin\delta + \cos\phi\cos\delta\cos h)\right) \tag{17}$$

with the latitude ϕ depending on the location, the solar declination $\delta = 0.405\sin\left(\frac{2\pi}{1\,\mathrm{y}}(t-91\,\mathrm{d})\right)\mathrm{rad}$ and the hour angle $h = \frac{2\pi}{1\,\mathrm{d}}t\ \mathrm{rad}$. The maximum possible irradiance from the sun at the ground at any point in time is $E_\mathrm{g} = \rho E_0$, with the solar constant $E_0 = 1362\,\mathrm{W/m^2}$ and the atmospheric proportion ρ as a design parameter. The final step of the transformation is the ratio (16)

$$\eta := \frac{1}{\exp(-\chi_{\mathcal{I}})+1} \tag{18}$$

which symmetrically maps values between $(-\infty, \infty)$ to values between $(0,\, 1)$.

For the temperature $\mathcal{T}$ we assume it to be normally distributed. This results in

$$\mathcal{T} = T_{\mathcal{T}}(\chi_{\mathcal{T}}) := \chi_{\mathcal{T}}. \tag{19}$$

We assume the wind speed to be Weibull distributed with the probability density function

$$f_\mathrm{W}(\mathcal{W}) = \lambda\kappa(\lambda\mathcal{W})^{\kappa-1}e^{-(\lambda\mathcal{W})^\kappa} \tag{20}$$

for positive wind speeds $\mathcal{W} > 0$. The time-variant colored wind speed noise signal $\chi_{\mathcal{W}}$ is entirely normally distributed with a probability density function

$$f_\mathrm{N}(\chi_{\mathcal{W}}) = \frac{1}{\sigma_\mathrm{N}\sqrt{2\pi}}\exp\left(-\frac{1}{2}\left(\frac{\chi_{\mathcal{W}}-\mu_\mathrm{N}}{\sigma_\mathrm{N}}\right)^2\right). \tag{21}$$

The constraint for the transformation (7) is that the probability for values lower than $\chi_{\mathcal{W}}$ equals the probability for values lower than $T_{\mathcal{W}}(\chi_{\mathcal{W}})$ which leads to

$$\begin{aligned}
&\int_{-\infty}^{\chi_{\mathcal{W}}} f_\mathrm{N}(\check{\chi}_{\mathcal{W}})\mathrm{d}\check{\chi}_{\mathcal{W}} \overset{!}{=} \int_{T_{\mathcal{W}}(-\infty)}^{T_{\mathcal{W}}(\chi_{\mathcal{W}})} f_\mathrm{W}(\check{\mathcal{W}})\mathrm{d}\check{\mathcal{W}}\\
\Rightarrow\quad \mathcal{W} &= \frac{1}{\lambda}\sqrt[\kappa]{\ln\left(\frac{1}{2}-\frac{1}{2}\,\mathrm{erf}\left(\frac{\chi_{\mathcal{W}}-\mu_\mathrm{N}}{\sqrt{2}\sigma_\mathrm{N}}\right)\right)} && (22)
\end{aligned}$$

with the Gauss error function erf. The remaining two degrees of freedom are resolved by

$$\mu_\mathrm{W} \approx \frac{1}{\lambda} \quad\Rightarrow\quad \lambda:\ \mu_\mathrm{N} = \frac{1}{\lambda} \tag{23}$$

$$\sigma_\mathrm{W} \approx \frac{1}{\kappa\lambda} \quad\Rightarrow\quad \kappa:\ \sigma_\mathrm{N} = \frac{1}{\lambda\kappa} \tag{24}$$

with the mean μ_W and standard deviation σ_W of the Weibull distribution.

B. Parameterize model: time series analysis

This section describes how to analyze measured data to obtain the model parameters. The measured irradiance $\hat{\mathcal{I}}$, temperature $\hat{\mathcal{T}}$ and wind speed $\hat{\mathcal{W}}$ are combined to the initial time series $\hat{x} = \begin{pmatrix}\hat{\mathcal{I}} & \hat{\mathcal{T}} & \hat{\mathcal{W}}\end{pmatrix}^T$. The analysis procedure is as follows:

1) Transformation to normally distributed time series: The first step is to compute the transformed data $\hat{\chi}_n$. This step is significantly different for the three different kinds of RERs.

The transformation of the **irradiance** to normally distributed data is based on (16) - (18). The transformation (16) $\mathcal{I}(t) = \eta\mathcal{I}_{\max}(t)$ has to be solved for η, with the challenge of the maximum actual irradiance $\mathcal{I}_{\max}(t)$ (17) being zero at night. This transformation is solved for the ratio η by

$$\hat{\eta}[t] = \frac{\hat{\mathcal{I}}[t]\mathcal{I}_{\max}(t)}{\mathcal{I}^2_{\max}(t)+\epsilon} \tag{25}$$

with a small number ϵ which causes $\hat{\eta}$ to get close to zero for $\mathcal{I}_{\max}$ getting close to zero. Values of the ratio $\hat{\eta}$ have only marginal influence on the final result for minor values of $\mathcal{I}_{\max}$.

The time-variant noise signal for the irradiance $\hat{\chi}_\mathcal{I}$ is computed by (18).

The transformation of the **temperature** is based on (19).

We assume the **wind speed** to be Weibull distributed. The exact distribution can be fitted by different approaches, we equal the arithmetic mean of the recorded data $\hat{\mathcal{W}}$ and the mean of the Weibull distribution, and both standard deviations. This leads to the scale parameter λ and the shape parameter κ. Through (22) we apply

$$\hat{\chi}_\mathcal{W} = \frac{1}{\lambda} + \frac{\sqrt{2}}{\lambda\kappa}\,\mathrm{erf}^{-1}\left(1 - 2e^{-(\lambda\hat{\mathcal{W}})^\kappa}\right). \tag{26}$$

2) Time-variance analysis: The following step is to analyze the time-variance of the normally distributed time series $\hat{\chi}_n$. The time-variances depend on the mean $\hat{\mu}_n[t]$ and the standard deviation $\hat{\sigma}_n[t]$ of the signals $\hat{\chi}_n[t]$ which are based on the values of one point in time t of several years. For this we distinguish between the irradiance and both other RERs. The irradiance data $\hat{\chi}_\mathcal{I}$ has no influence on the model for all $\mathcal{I}_\text{max} = 0$, at night. Only values at points in time $t_\mathcal{I}$ with $\mathcal{I}_\text{max}(t_\mathcal{I}) \neq 0$ are used to model the time-variance of the irradiance. This is solved by a numerical minimization problem, which includes a weight function

$$w = \min(\mathcal{I}_\text{max}, W_\text{max}) \tag{27}$$

with a constant design parameter W_max. The parameter set $\underline{p}_{\mathcal{I}z}$ containing the Fourier parameters of the irradiance, is computed out of the function $z_\mathcal{I}(t;\underline{p}_{\mathcal{I}z})$ which represents the first vector element of (12) respectively. The numerical minimization problem results in

$$\underline{p}_{\mathcal{I}z} = \underset{p'_{\mathcal{I}z}}{\arg\min}\left\{\sum_t w(t)\cdot\left(\hat{z}_\mathcal{I}[t] - z_\mathcal{I}(t;\underline{p}'_{\mathcal{I}z})\right)^2\right\}, \tag{28}$$

which fits the mean or the standard deviation of the irradiance.

The wind speed's and the temperature's mean and standard deviations z_n are modeled by a first order Fourier series approximation with the parameter set $\underline{p}_{nz}$ determined by Fourier series, as no weight functions are useful. First, we apply a Fourier series on each day of a year with a base frequency of $\omega^\text{d} = \frac{\pi}{12\,\text{h}}$ and afterwards we apply a Fourier series on the resulting time-variant Fourier parameters for the entire year, with a base frequency of $\omega^\text{y} = \frac{\pi}{4230\,\text{h}}$ resulting in the parameter vector $\underline{p}_{nz}$. From this we compute through (12) - (15) the modeled mean $\hat{\mu}_n[t]$ and standard deviation $\hat{\sigma}_n[t]$, which we apply through (3) to $\hat{\chi}_n$, to obtain the correlated $\mathcal{N}(0,1)$-noise samples $\hat{\chi}''_n$.

3) Spectrum analysis: The spectrum analysis, is based on a discrete Fourier transform. The amplitude spectrum of the filter (9) is fit to the resulting amplitude spectrum of $\hat{\chi}''_n$ which finally leads to the time constants T_n. The time constant leads to the filter gain B_n (11), so that it does not affect the overall signal energy and hence the $\mathcal{N}(0,1)$-distribution.

4) Causal dependency analysis: The last remaining parameter ζ_n, which models the correlation between the RERs is determined. For this, we apply the dynamics $\frac{G_\mathcal{I}}{G_\mathcal{T}}$ on the temperature signal $\hat{\chi}''_\mathcal{T}$ to consider phase transitions due to the dynamics G_n. For the wind speed we apply $\frac{G_\mathcal{T}}{G_\mathcal{W}}$, to compare it with the temperature. The correlation parameter ζ_n is computed through the covariance of $\hat{\chi}''_{nG} := \frac{G_{n-1}}{G_n}\hat{\chi}''_n$ and $\hat{\chi}''_{n-1}$ resulting in

$$\begin{aligned}\mathrm{cov}(\hat{\chi}''_{nG}, \hat{\chi}''_{n-1}) &= \mathrm{E}(\hat{\chi}''_{nG}\cdot\hat{\chi}''_{n-1}) \overset{!}{=} \frac{\zeta_n}{\zeta_n + 1}\\ \Rightarrow\quad \zeta_n &= \frac{\mathrm{cov}(\hat{\chi}''_{nG}, \hat{\chi}''_{n-1})}{1 - \mathrm{cov}(\hat{\chi}''_{nG}, \hat{\chi}''_{n-1})}\end{aligned}$$

for $n \in \{\mathcal{T}, \mathcal{W}\}$ and $n-1 \in \{\mathcal{I}, \mathcal{T}\}$. For computing the covariance between the wind speed and the temperature, we consider each point in time. For computing the covariance of the temperature and the irradiance, we consider all points in time $t_\mathcal{I} : \mathcal{I}_\text{max} > 0$ to avoid to consider the artificial values of the ratio, which are introduced to avoid the division by zero in (25).

TABLE I
WEATHER MODEL PARAMETERS OF GARCHING

$T_\mathcal{I}$	30 h	ρ	0.9		
$A_{0A0\mu\mathcal{I}}$	−0.72	$A_{1A0\mu\mathcal{I}}$	0.19	$\varphi_{1A0\mu\mathcal{I}}$	0.95 rad
$A_{0A1\mu\mathcal{I}}$	−0.66	$A_{1A1\mu\mathcal{I}}$	0.66	$\varphi_{1A1\mu\mathcal{I}}$	−0.36 rad
$A_{0\varphi1\mu\mathcal{I}}$	−0.72	$A_{1\varphi1\mu\mathcal{I}}$	0.19	$\varphi_{1\varphi1\mu\mathcal{I}}$	0.95 rad
$A_{0A0\sigma\mathcal{I}}$	1.24	$A_{1A0\sigma\mathcal{I}}$	0.19	$\varphi_{1A0\sigma\mathcal{I}}$	0.90 rad
$A_{0A1\sigma\mathcal{I}}$	−0.12	$A_{1A1\sigma\mathcal{I}}$	0.09	$\varphi_{1A1\sigma\mathcal{I}}$	−0.04 rad
$A_{0\varphi1\sigma\mathcal{I}}$	0.13	$A_{1\varphi1\sigma\mathcal{I}}$	−1.78	$\varphi_{1\varphi1\sigma\mathcal{I}}$	−0.86 rad
$T_\mathcal{T}$	30 h	$\zeta_\mathcal{T}$	0.59		
$A_{0A0\mu\mathcal{T}}$	7.89	$A_{1A0\mu\mathcal{T}}$	9.49	$\varphi_{1A0\mu\mathcal{T}}$	−2.79 rad
$A_{0A1\mu\mathcal{T}}$	3.18	$A_{1A1\mu\mathcal{T}}$	1.57	$\varphi_{1A1\mu\mathcal{T}}$	−3.06 rad
$A_{0\varphi1\mu\mathcal{T}}$	−2.32	$A_{1\varphi1\mu\mathcal{T}}$	0.29	$\varphi_{1\varphi1\mu\mathcal{T}}$	0.19 rad
$A_{0A0\sigma\mathcal{T}}$	4.12	$A_{1A0\sigma\mathcal{T}}$	1.02	$\varphi_{1A0\sigma\mathcal{T}}$	0.57 rad
$A_{0A1\sigma\mathcal{T}}$	0.91	$A_{1A1\sigma\mathcal{T}}$	0.33	$\varphi_{1A1\sigma\mathcal{T}}$	2.57 rad
$A_{0\varphi1\sigma\mathcal{T}}$	−0.48	$A_{1\varphi1\sigma\mathcal{T}}$	1.26	$\varphi_{1\varphi1\sigma\mathcal{T}}$	−0.14 rad
$T_\mathcal{W}$	20 h	$\zeta_\mathcal{W}$	0.23	ϵ	0.001
$A_{0A0\mu\mathcal{W}}$	2.61	$A_{1A0\mu\mathcal{W}}$	0.59	$\varphi_{1A0\mu\mathcal{W}}$	0.95 rad
$A_{0A1\mu\mathcal{W}}$	0.77	$A_{1A1\mu\mathcal{W}}$	0.30	$\varphi_{1A1\mu\mathcal{W}}$	3.06 rad
$A_{0\varphi1\mu\mathcal{W}}$	−1.16	$A_{1\varphi1\mu\mathcal{W}}$	0.98	$\varphi_{1\varphi1\mu\mathcal{W}}$	−0.34 rad
$A_{0A0\sigma\mathcal{W}}$	1.36	$A_{1A0\sigma\mathcal{W}}$	0.49	$\varphi_{1A0\sigma\mathcal{W}}$	0.44 rad
$A_{0A1\sigma\mathcal{W}}$	−0.05	$A_{1A1\sigma\mathcal{W}}$	−0.03	$\varphi_{1A1\sigma\mathcal{W}}$	−2.38 rad
$A_{0\varphi1\sigma\mathcal{W}}$	−0.16	$A_{1\varphi1\sigma\mathcal{W}}$	−0.66	$\varphi_{1\varphi1\sigma\mathcal{W}}$	−0.99 rad

Units: $\mathcal{I}$ in $\mathrm{W/m^2}$, $\mathcal{T}$ in °C, $\mathcal{W}$ in $\mathrm{m/s}$

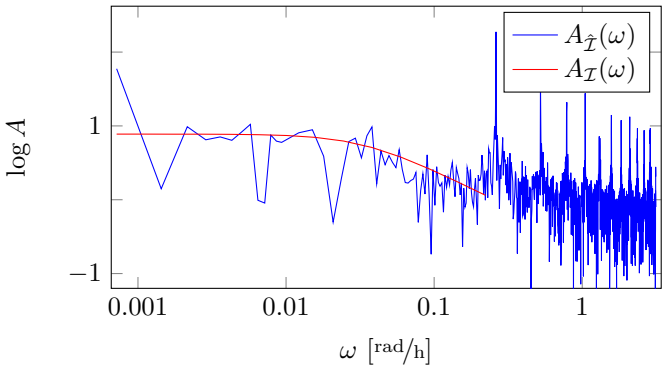

Fig. 1. Displays the spectrum of the irradiance noise signal for the recorded (with hat) and the synthesized data, with the peaks of one day and its harmonics.

IV. Experimental Evaluation

This section describes a case scenario of modeling global horizontal irradiance $\mathcal{I}$, air temperature $\mathcal{T}$ and wind speed $\mathcal{W}$

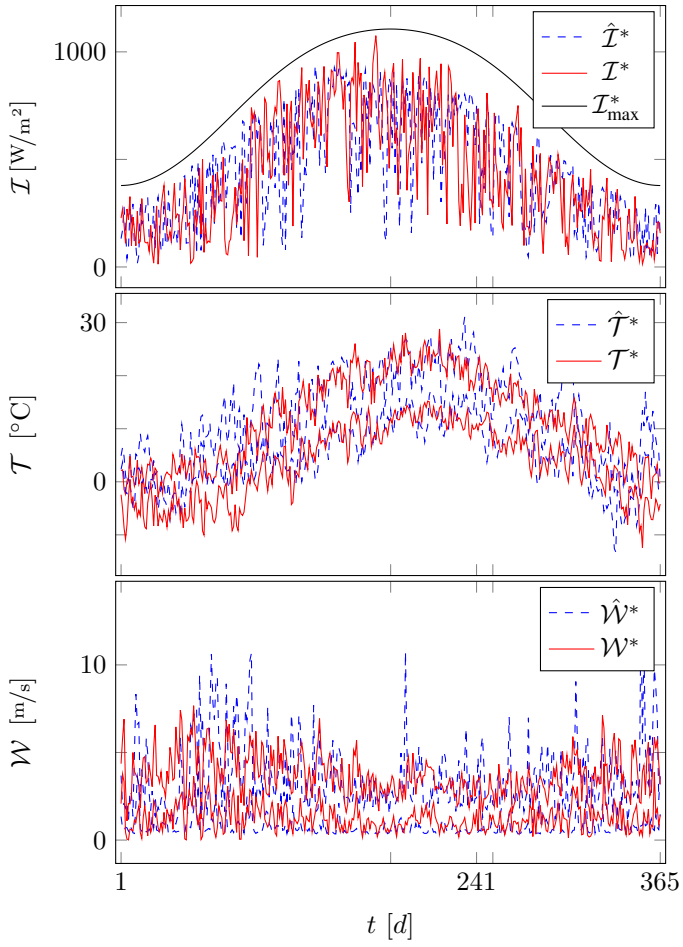

Fig. 2. Illustrates the maximum and the minimum value of each one day, for one year, for the global horizontal irradiance $\mathcal{I}$, the air temperature $\mathcal{T}$ and the wind speed $\mathcal{W}$. The upper index $*$ indicates that only the maximum/minimum of each day is plotted. The measured samples are written with a hat.

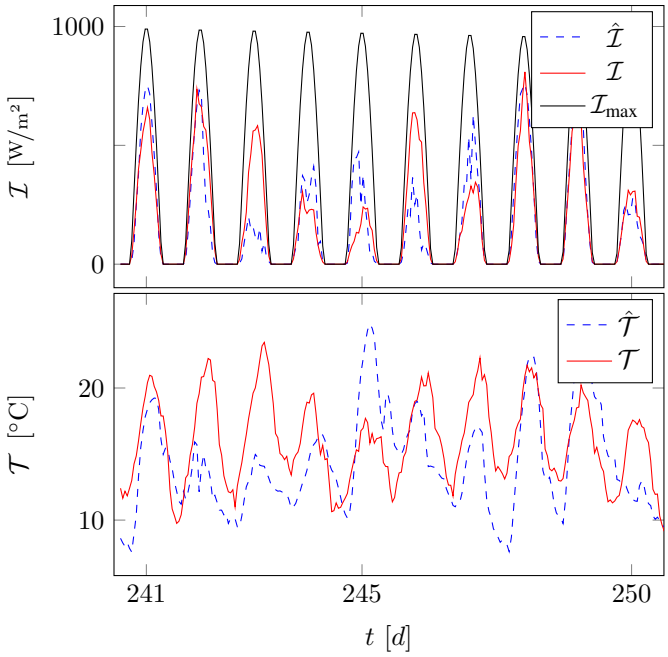

Fig. 3. Illustrates a detailed view of day 241 to 250 of the irradiation $\mathcal{I}$ and the temperature $\mathcal{T}$ for the recorded (with hat) and the synthesized data.

TABLE II
OVERALL ACCURACY

n	μ_n	$\hat{\mu}_n$	σ_n	$\hat{\sigma}_n$
$\mathcal{I}$ in W/m²	129.70	128.24	212.40	210.63
$\mathcal{T}$ in °C	7.89	7.89	7.94	8.39
$\mathcal{W}$ in m/s	2.35	2.30	1.25	1.83

10 m above ground level of Garching, Germany. First we apply the analysis algorithm as described in Sec. III-B. The resulting parameters are listed in Tab. I.

The resulting spectrum of the correlated $\mathcal{N}(0,1)$-noise samples $\hat{\chi}''_n$ is exemplary for the irradiance illustrated in Fig. 1. We observe disturbances and spikes for periods smaller than one day ($\omega > 0.26\,\mathrm{rad/h}$). The filter time constant T_n is determined to minimize the difference between the spectrum of the filter and of the recorded time series until periods of one day.

The model, which is parameterized by the time series analysis results in the synthesized time series $\mathcal{I}$, $\mathcal{T}$ and $\mathcal{W}$. Its minimum and maximum values throughout each day, as well as the recorded time series are illustrated in Fig. 2. We observe the typical seasonal behavior, higher irradiance and temperature in the summer and higher wind speeds in the winter. The recorded wind speeds show some spikes, e.g. at day 193, which are not obtained by the model. There is a tendency for higher temperatures of the recorded data from day 50 to day 120, which exists only in the recorded data of the illustrated year. Besides this, throughout numerous experiments we could not observe any further significant differences between the recorded and the synthesized time series.

A detailed view into the time series is given in Fig. 3 which illustrates the time series between day 241 and 250 with an hourly resolution for the synthesized and the recorded time series. Regarding the diurnal variation, there are lower temperatures and zero irradiance at night, for the synthesized and the recorded data. We observe in day 244 and 245 a drop of the irradiance and temperature of the synthesized time series. During day 247, we obtain a lower irradiance without temperature change, in comparison with the day before and afterwards for the synthesized time series. The recorded time series have during day 243 to 246 a substandard low irradiance, but at day 245 an outstanding high temperature.

The overall accuracy of the entire analysis and modeling process is measured by comparing the overall mean and standard deviation of the entire time series. The overall mean and standard deviation of the synthesized (μ_n, σ_n) and of the recorded time series ($\hat{\mu}_n$, $\hat{\sigma}_n$) are listed in Tab. II. The relative mean deviation of the recorded data is for the mean 1.1% and for the standard deviation 12.6%.

V. Discussion

This section discusses the model with its results of Sec. IV. The overall evaluation of the modeling quality is high. Significant sources for inaccuracies are the approximation of the overall distribution functions and the first harmonics approximation of the time-variances.

The data analysis results in the spectrum of the correlated $\mathcal{N}(0,1)$-noise samples $\hat{\chi}_n''$ with significant errors for periods up to one day. The main error source is the inaccuracy due to the first harmonics approximation of the time-variances. These harmonics are not completely compensated and hence appear in this spectrum. Compensating the ideal time-variances leads to most errors to disappear, except for the irradiance. The spikes of the irradiance spectrum in this frequency space are caused by having no measured values at night. These gaps are finally filled with zero by the above described mathematics, which causes disturbances in this frequency space, with spikes at the period of one day and its higher harmonics. The resulting synthesized time series show a similar behavior as the recorded reference time series. The mathematics of the modeling ensure the similar frequency spectrum, as long as the recorded data are possible to model with a first order system. We obtain some extreme wind speeds in the recorded data which are not correctly reproduced by the model. This causes the worse overall accuracy of the standard deviation and the only significant difference between modeled and measured data, which could be observed during experiments with this reference data set.

In the detailed view, we obtain that the temperature follows in general the irradiance. Due to the stochastic behavior of the model, there are still deviations from this behavior, as during day 247. Such outliers can also be found in the recorded data, e.g. during day 245.

VI. Conclusion

This paper investigates the modeling of weather phenomena which are interpreted as renewable energy resources. The approach includes the time-variance, realistic rates of change and the causality relation of the RERs. The model is continuous with a simple analytical description.

The methodology of this work distinguishes a general concept and a specific application. The general concept is without significant sources for errors, but with an infinite complexity. Specific applications introduce approximations which cause deviations from the ideal behavior. The major approximations of the presented specific application are the dynamical behavior of a first order system, approximating the time-variances by its first order harmonics and the assumption of data fitting to specific distribution functions.

The resulting model applies to different tasks. The model is useful for generating long time series, for instance for Monte Carlo simulations or in case of data sparsity. It is possible to investigate the effect of climate change by adapting the model parameters. A major chance is to use this model for new analytical analysis methods.

In the future work we plan to simplify the model and reduce the parameter set. We plan to develop transformations to be able to generate the model parameter set from few graspable parameters.

Acknowledgment

The authors would like to thank H. Loesslein from the Meteorological Institute Munich for providing the reference data.

References

[1] P. Ailliot, D. Allard, P. Naveau, C. D. Beaulieu, and R. Cedex, "Stochastic weather generators : an overview of weather type models," pp. 1–14, 2015.

[2] G. Papaefthymiou and B. Kl, "MCMC for Wind Power Simulation," vol. 23, no. 1, pp. 234–240, 2008.

[3] S. Apipattanavis, G. Podesta, B. Rajagopalan, and R. W. Katz, "A semiparametric multivariate and multisite weather generator," vol. 43, no. 2, 2007.

[4] R. Billinton, "Consideration of Multi-State Weather Models in Realiability Evaluation of Transmission and Distribution System." no. May, pp. 619–622, 2005.

[5] S. Talari, M. Yazdaninejad, and M.-r. Haghifam, "Stochastic-based scheduling of the microgrid operation including wind turbines , photovoltaic cells, energy storages and responsive loads," vol. 9, pp. 1498–1509, 2015.

[6] E. A. Mohamed and Y. G. Hegazy, "A Novel Probablistic Strategy for Modeling Photovoltaic Based Distributed Generators," vol. 9, no. 8, pp. 864–867, 2015.

[7] K. Roe, D. Stevens, and C. Mccord, "High Resolution Weather Modeling for Improved Fire Management," no. November, 2001.

[8] M. B. Parlange and R. W. Katz, "An Extended Version of the Richardson Model for Simulating Daily Weather Variables," pp. 610–622, 2000.

[9] J. E. Hay, "Calculating solar radiation for inclined surfaces: Practical approaches," *Renewable Energy*, vol. 3, no. 4-5, pp. 373–380, 1993.